Dissipation Loss Effects in Isolated and Coupled Transmission Lines

BARRY E. SPIELMAN, MEMBER, IEEE

Abstract—**This paper describes a computer-aided analysis of dissipation losses in uniform isolated or coupled transmission lines for microwave and millimeter-wave integrated-circuit applications. The analysis employs a quasi-TEM model for isolated transmission lines and for the even- and odd-mode transmission lines associated with coupled-line structures. The conductor and dielectric losses are then related to equivalent charge density distributions, which are evaluated using a method-of-moments solution. The transmission lines treated by this analysis may contain any number of lossy conductors and inhomogeneous dielectrics, consisting of any number of different homogeneous dielectric regions. A development is provided to explicitly relate the four-port terminal-electrical performance of directional couplers to evaluated even- and odd-mode loss coefficients.**

Examples of evaluated losses are presented in graphical form for isolated lines of inverted microstrip and trapped inverted microstrip and edge-coupled microstrip with a dielectric overlay. The analysis accuracy has been confirmed using microstrip and coplanar waveguide configurations. A comparison is made of the total loss characteristics for microstrip, coplanar waveguide, inverted microstrip, and trapped inverted microstrip. Calculations are compared with measurements for the coupled-line structure. Accuracy of the solution and suggested refinements are discussed. Five computer programs are documented.

I. Introduction

THERE is considerable interest in investigating and exploiting new transmission lines for use in integrated circuits operating at higher microwave and millimeter-wave frequencies. This interest has been spurred by the success in effecting reductions in circuit cost, size, and weight through the application of microstrip at lower to intermediate microwave frequencies. Unfortunately, microstrip is discouragingly lossy and more difficult to fabricate at higher microwave and millimeter-wave frequencies. These considerations have prompted the search for transmission lines that are amenable to integrated-circuit fabrication methods (thin-film and photolithographic technology) and which have improved loss characteristics compared with microstrip.

To facilitate the investigation of transmission lines which offer potential for improvements over microstrip at the frequencies of interest, a flexible computer-aided analysis of transmission-line losses has been implemented. This analysis is suitable for application to a wide variety of transmission lines. This paper describes the implementation of that analysis as it applies to both isolated and coupled transmission lines, where losses due to both conductor and dielectric dissipation are taken into account. Various examples of loss evaluations using this formulation are presented for both isolated and coupled transmission lines of interest.

Manuscript received August 23, 1977; revised January 19, 1977.

The author is with the Microwave Techniques Branch, Electronics Technology Division, Naval Research Laboratory, Washington, DC 20375.

II. Formulation of Analysis for Evaluation of Losses

The approach used here for the analysis of conductor and dielectric loss characteristics of isolated or coupled uniform transmission lines is consistent with the quasi-TEM models described in [1] and [2]. For isolated transmission lines, the direction of propagation is taken to be along the z direction. Consistent with the quasi-TEM model and the transmission-line wave approach described in [3], the z dependence for voltage and current along the transmission line conductor and dielectric loss coefficients α_c and α_d, α is the attenuation constant due to conductor and dielectric losses and β is the phase constant. Following the development set forth in [3], the attenuation constant α is given by

$$\alpha = \bar{P}_d/(2\bar{P}_f) \tag{1}$$

where $\bar{P}_d$ is the time-averaged power dissipated per unit length and $\bar{P}_f$ is the time-averaged power flow along line.

In the following portion of this paper, explicit expressions are developed for use in evaluating isolated transmission-line conductor and dielectric loss coefficients α_c and α_d, respectively. The total coefficient α is obtained from these by summing α_c and α_d.

A. Isolated Transmission Lines

To obtain a useful expression for $\bar{P}_f$ in (1) a development, the details of which are found in [4], is summarized as follows. The complex flow P_f is represented in terms of a $+z$ traveling wave on a lossy transmission line. ReZ_0 and $|Z_0|$ are approximated [4] by $(Z_0)_{LL}$, the characteristic impedance of the same line without losses. By virtue of these considerations $\bar{P}_f$ can be expressed as

$$\bar{P}_f = |V_0|^2 vCe^{-2\alpha z} \tag{2}$$

where v is the phase velocity, C is the electrostatic capacitance per unit length, and $|V_0|^2$ is the amplitude squared of the wave voltage at $z = 0$.

1) Conductor Losses: To obtain an expression which is useful for evaluating $\bar{P}_d$ in (1) for losses due to imperfect conductors, the approximation described in [5] is employed. $\bar{P}_d$ can be expressed approximately by

$$\bar{P}_{d,c} = \int |H_0|^2 R \, dl. \tag{3}$$

Here, $|H_0|^2$ is the amplitude squared of the magnetic field at conducting surfaces for the lossless case. R is the surface

resistance of the metals in the system. Here, the additional subscript "c" on $\bar{P}_{d,c}$ denotes power losses due to imperfect conductors. For good conductors, R is expressed [6] in terms of frequency f, free-space permeability μ_0, and dc conductivity σ. Using the quasi-TEM propagation assumption, $|H_0|^2$ is related to $|E_0|^2$, where $\bar{E}_0$ is the electric field in the lossless medium [4].

In the lossless TEM solution described in [1] and [2], the electric field in a medium with permittivity ε, the electric field at a point along the surface of a perfect conductor, is given by

$$E_0 = 2\pi q \tag{4}$$

where q is a flux-source distribution residing at the conductor surface and $2\pi\varepsilon q$ can be thought of as the equivalent charge-density distribution (sum of free and polarization charge densities). In [1], the flux-source distribution residing along the surface of the N_jth conductor, in a system having a total of N_c conductor surfaces, is approximated by a pulse expansion as

$$q^{N_j} = \sum_{i=1}^{(N_S)_j} q_i^{N_j} P^{N_j}(i), \qquad N_j = 1, \cdots, N_c. \tag{5}$$

This representation arises by subdividing the contour defined by the surface of the N_jth conductor into $(N_S)_j$ segments. Along the ith segment the free charge-density distribution is taken to be constant at the value $q_i^{N_j}$. $P(i)$ is a pulse function defined by

$$P^{N_j}(i) = \begin{cases} 1, & \text{on the } i\text{th section of } N_j \\ 0, & \text{on all other sections of } N_j. \end{cases} \tag{6}$$

Then, rewriting $\bar{P}_{d,c}$ in (3) and using (1), (2), (4)–(6), the loss coefficient due to conductor losses α_c can be written as

$$\alpha_c \approx \frac{20}{\ln 10} \cdot \frac{2\pi^2 \varepsilon_0 \varepsilon_{\text{eff}} \sqrt{\frac{\pi f \mu_0}{\sigma}}}{\mu_0 |V_0|^2 vC} \cdot \sum_{j=1}^{N_c} \sum_{i=1}^{(N_S)_j} (q_i^{N_j})^2 \Delta l_i^{N_j} \quad \text{dB/unit length} \tag{7}$$

where $\Delta l_i^{N_j}$ is the length of the ith segment on the N_jth conductor, ε_0 is the permittivity of free space, and ε_{eff} is given by

$$\varepsilon_{\text{eff}} = \frac{C}{C_0}. \tag{8}$$

Here, C_0 is the electrostatic capacitance of the transmission line under consideration, but with all dielectric materials fictitiously removed. It is the expression given in (7) which is embodied in the computer programs described in [4]. This expression has been used to provide the design information for conductor losses found in Section III.

2) *Dielectric Losses:* To obtain an expression which is useful for evaluating $\bar{P}_d$ in (1) for losses due to imperfect dielectrics, this quantity is initially written as

$$\bar{P}_{d,d} = \sum_{i=1}^{N_D} \int_{A_i} \omega \varepsilon_0 \varepsilon_i'' |E|^2 \, dS. \tag{9}$$

Here, the second subscript "d" on $\bar{P}_{d,d}$ denotes that the dissipation losses are due to imperfect dielectrics. N_D is the number of imperfect dielectric regions where the ith region has a complex permittivity given by $\varepsilon_i = \varepsilon_0(\varepsilon_i' - j\varepsilon_i'')$. A_i represents the area, in the transmission-line cross section, spanned by the ith simply connected homogeneous lossy dielectric region. Equation (9) can be rewritten as

$$\bar{P}_{d,d} = \sum_{i=1}^{N_D} \int_{A_i} \omega \tan \delta_i W_{ei} \, dS \tag{10}$$

where $\tan \delta_i$ is the loss tangent of the material in the ith region. The time-averaged energy stored in the electric field in the ith dielectric region is given by

$$\bar{W}_{ei} = \tfrac{1}{2} \int_{A_i} \varepsilon_0 \varepsilon_i' |E|^2 \, dS. \tag{11}$$

In [4] details of a development are presented which show that the time average of the total energy stored in the electric field per unit length of transmission line $\bar{W}_e$ is related to $\bar{W}_{ei}$ by

$$\bar{W}_{ei} = \varepsilon_i \frac{\partial \bar{W}_e}{\partial \varepsilon_i}. \tag{12}$$

While the development in [4] provides a general result for transmission structures with many conductors and dielectrics over the cross section, for isolated lines or coupled lines treated by an even- and odd-mode two-port interpretation $\bar{W}_e$ can be expressed as

$$\bar{W}_e = \tfrac{1}{2} C |V|^2 \tag{13}$$

where C is the electrostatic capacitance of the transmission line in the two-port configuration (isolated and even- or odd-mode line) and V is the voltage associated with a $+z$ traveling wave on the line.

To facilitate the evaluation of a dielectric loss coefficient in terms of readily computable parameters, equations (1), (2), (8), and (10)–(13) are combined to provide the following expression:

$$\alpha_d = \frac{20\pi f}{\ln 10 \, c\sqrt{\varepsilon_{\text{eff}}}} \sum_{i=1}^{N_D} \varepsilon_i' \tan \delta_i \frac{\partial \varepsilon_{\text{eff}}}{\partial \varepsilon_i'} \quad \text{dB/unit length.} \tag{14}$$

In (14), c is the speed of light in free space. To evaluate the partial derivative in (14) a "forward" difference quotient is employed, providing the computationally useful result

$$\alpha_d = \frac{20\pi f}{\ln 10 \, c\sqrt{\varepsilon_{\text{eff}}}} \sum_{i=1}^{N_D} \varepsilon_i' \tan \delta_i \left(\frac{\hat{\varepsilon}_{\text{eff}} - \varepsilon_{\text{eff}}}{\hat{\varepsilon}_i' - \varepsilon_i'} \right) \quad \text{dB/unit length.} \tag{15}$$

In (15) $\hat{\varepsilon}_{\text{eff}}$ is the value of ε_{eff} for the structure under consideration when the value of the permittivity for the ith homogeneous dielectric region is perturbed to a slightly different (higher) value $\hat{\varepsilon}_i'$. It is this expression which has been incorporated into the computer programs which are documented in [4]. For these programs the index "i" takes the value of "1" since there is only one lossy homogeneous-dielectric region in the overall inhomogeneous structures treated by the computer programs.

B. Coupled Transmission-Line Structures

For the purposes of this section the coupled transmission lines will be treated by an even- and odd-mode interpretation [7]. Although two transmission lines coupled over a given length truly represents a four-port structure, the even- and odd-modes associated with this structure are each two-port transmission lines which can be treated separately. To properly assess the effects of losses in such structures the problem is twofold. One problem is to determine the loss coefficients α_c and α_d for each of the even and odd modes. The second problem is to determine the effects of these coefficients on the four-port terminal-electrical performance of the entire structure. In the material to follow the former problem will be discussed first and will be followed by a treatment of the latter problem explicitly for four-port directional coupler loss effects.

1) Even- and Odd-Mode Loss Coefficients: Since the even- and odd-modes for a coupled line structure can each be depicted as two-port transmission lines whose length is that of the coupled-line region, the loss coefficients for conductor and dielectric losses can be determined using (7) and (15), respectively. The even- and odd-mode loss coefficients for losses due to imperfect conductors can be written as

$$\alpha_{ck} \approx \frac{20}{\ln 10} \cdot \frac{2\pi^2 \varepsilon_0 (\varepsilon_{\text{eff}})_k}{\mu_0 |V_0|^2 v_k C_k} \sqrt{\frac{\pi f \mu_0}{\sigma}} \cdot \sum_{j=1}^{NC} \sum_{i=1}^{(Ns)j} (q_{ik}^{Nj})^2 \Delta l_{ik}^{Nj} \quad \text{dB/unit length} \quad (16)$$

where $k = e$ for the even mode and $k = o$ for the odd mode. The quantities v_k, C_k, q_{ik}, $(\varepsilon_{\text{eff}})_k$, and Δl_{ik} are evaluated as described in [1]. The expression for even- and odd-mode loss coefficients for losses due to imperfect dielectrics can be expressed as

$$\alpha_{dk} \approx \frac{20\pi f}{\ln 10\, c \sqrt{(\varepsilon_{\text{eff}})_k}} \sum_{i=1}^{ND} \varepsilon_i' \tan \delta_i \cdot \left[\frac{(\hat{\varepsilon}_{\text{eff}})_k - (\varepsilon_{\text{eff}})_k}{\hat{\varepsilon}_i' - \varepsilon_i'} \right] \quad \text{dB/unit length} \quad (17)$$

where $k = e$ for the even mode and $k = o$ for the odd mode. In (17) $(\varepsilon_{\text{eff}})_k$ represents the effective relative permittivity for the even- or odd-mode in the coupled-line configuration to be analyzed. This value is determined using the method described explicitly in [1]. $(\hat{\varepsilon}_{\text{eff}})_k$ is evaluated the same way for the coupled-line structure where the relative permittivity of the ith dielectric region ε_i' is perturbed to the slightly higher value $\hat{\varepsilon}_i'$. Equations (16) and (17) have been used to evaluate the even- and odd-mode conductor and dielectric loss coefficients for the coupled-line structures described in Section III of this paper. The total loss coefficients α_e and α_o for the even- and odd-modes are obtained by adding the respective values of α_{ck} and α_{dk}.

2) Effects of Losses on Four-Port Terminal Performance: An understanding of the effects of losses on the four-port terminal performance of directional couplers is facilitated by considering the following. The problem at hand is one of determining the loss effects on measurable terminal voltages b_i $(i = 1,2,3,4)$, leaving these ports, once the loss coefficients $(\alpha_{ce}, \alpha_{de})$ and $(\alpha_{co}, \alpha_{do})$ have been determined for the modal transmission lines, respectively. These loss coefficients are assumed to be known for this development, having been computed by the method described in the previous section.

The approach used here starts with a procedure similar to that described in [7]. The voltage b_i $(i = 1,2,3,4)$ is written in terms of a sum or difference of Γ_{oe} and Γ_{oo} or T_{oe} and T_{oo} where (Γ_{oe}, T_{oe}) and (Γ_{oo}, T_{oo}) are pairs of reflection and transmission coefficients for the even- and odd-mode two ports, respectively. The reflection coefficients for the even or odd mode can be expressed in terms of the even- or odd-mode *ABCD* two-port network parameters [7]. The *ABCD* parameters for the lossy even- or odd-mode two-port are given by

$$A_i = D_i = \cosh \gamma_i l \quad (18)$$

$$B_i = Z_{0i} \sin \gamma_i l \quad (19)$$

$$C_i = \left(\frac{1}{Z_{0i}} \right) \sin \gamma_i l \quad (20)$$

where $i = e$ for the even mode and $i = o$ for the odd mode. In (18)–(20) *l represents the physical length of the coupled-line region;* Z_{0e} and Z_{0o} are the characteristic impedances of the even- and odd-mode transmission lines, respectively. γ_e and γ_o are the even- and odd-mode propagation constants, taken for this development to be given by

$$\gamma_e = \alpha_e + j\beta_e \quad (21)$$

$$\gamma_o = \alpha_o + j\beta_o \quad (22)$$

where α_e and α_o are the total (known) even- and odd-mode loss coefficients. β_e and β_o are the even- and odd-mode phase constants (known), respectively, which are determined by the lossless analysis described in detail in [1]. It is to be noted that the generality of this development permits β_e and β_o to be determined to allow for even and odd modes having different phase velocities.

Employing (18)–(20) the measurable terminal voltages of the four-port coupler under consideration can be expressed as follows:

$$b_2 = b_c = F_2 \left[\frac{\tanh \gamma_e l}{2 + F_1 \tanh \gamma_e l} + \frac{\tanh \gamma_o l}{2 + F_1 \tanh \gamma_o l} \right] \quad (23)$$

$$b_4 = b_t = \frac{\operatorname{sech} \gamma_e l}{2 + F_1 \tanh \gamma_e l} + \frac{\operatorname{sech} \gamma_o l}{2 + F_1 \tanh \gamma_o l} \quad (24)$$

$$b_3 = b_i = \frac{\operatorname{sech} \gamma_e l}{2 + F_1 \tanh \gamma_e l} - \frac{\operatorname{sech} \gamma_o l}{2 + F_1 \tanh \gamma_o l} \quad (25)$$

$$b_1 = b_r = F_2 \left[\frac{\tanh \gamma_e l}{2 + F_1 \tanh \gamma_e l} - \frac{\tanh \gamma_o l}{2 + F_1 \tanh \gamma_o l} \right] \quad (26)$$

where the subscripts c, t, i, and r denote coupled, transmitted, isolated, and reflected signals, respectively. In (23)–(26) F_1 and F_2 are quantities given by

$$F_1 \equiv \left(\frac{Z_{0e}}{Z_{0o}} \right)^{1/2} + \left(\frac{Z_{0o}}{Z_{0e}} \right)^{1/2} \quad (27)$$

$$F_2 \equiv \frac{1}{2} \left[\left(\frac{Z_{0e}}{Z_{0o}} \right)^{1/2} - \left(\frac{Z_{0o}}{Z_{0e}} \right)^{1/2} \right]. \quad (28)$$

For the special case where $\beta_e l = \beta_o l = \pi/2$, equations (21)–(26) simplify to become the following:

$$b_c = F_2 \left[\frac{1}{2\alpha_e l + F_1} + \frac{1}{2\alpha_o l + F_1} \right] \tag{29}$$

$$b_t = -j \left[\frac{1}{2\alpha_e l + F_1} + \frac{1}{2\alpha_o l + F_1} \right] \tag{30}$$

$$b_i = -j \left[\frac{1}{2\alpha_e l + F_1} - \frac{1}{2\alpha_o l + F_1} \right] \tag{31}$$

$$b_r = F_2 \left[\frac{1}{2\alpha_e l + F_1} - \frac{1}{2\alpha_o l + F_1} \right]. \tag{32}$$

It is to be noted that in (29)–(32) the even- and odd-mode loss coefficients appear explicitly. Also, it is easily seen from these relationships that, even for perfectly matched couplers, for α_e different from α_o the isolated and reflected signals are not zero. This effect is described quantitatively in Section IV. For couplers with other sources of impedance match and isolation degradation (e.g., different even- and odd-mode phase velocities) the additional degradation of isolation and reflected signal due to different modal loss characteristics will be superimposed on the other effects. The relationships developed in this section have been tested on experimental coupler models. The results are described in Section III.

III. Examples of Loss Evaluations and Design Information

In this section results are presented for specific isolated and coupled transmission-line structures. The accuracy of the analysis described in this paper has been confirmed [4] by comparing results calculated for microstrip and coplanar waveguide with well-accepted reference values. The results presented in the following sections for inverted microstrip and trapped inverted microstrip serve to provide useful currently unavailable design information for more complicated structures which offer potential for circuit applications. Following these results is a comparison of the loss characteristics for the four preceding transmission lines. The results for the edge-coupled microstrip structure with a dielectric overlay serve to confirm the utility of the coupled-line loss analysis described in Section II and to provide currently unavailable design information for this structure. This structure is presently the most viable approach for providing high-performance broad-band couplers, filters, and Schiffman phase-shift sections in a microstrip-compatible format [8].

A. Isolated Transmission Lines

1) Inverted Microstrip: The generic cross section of inverted microstrip is depicted in Fig. 1. Analyzed results for conductor and dielectric loss coefficients are shown in Fig. 2. The substrate dielectric constant chosen for this study corresponds to that of fused silica, which is deemed to be a suitable material for this transmission line at higher microwave and millimeter-wave frequencies. The characteristic impedance and phase velocities for the range of configurations treated in Fig. 2 are shown in Fig. 3 [4].

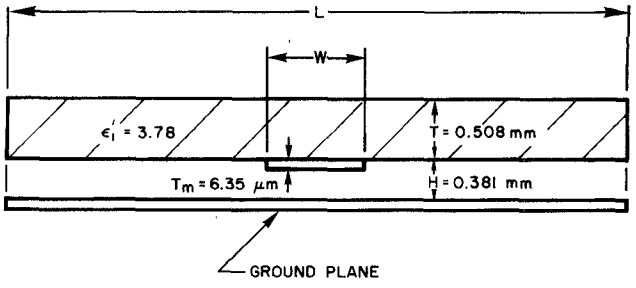

Fig. 1. Generic cross section of inverted microstrip.

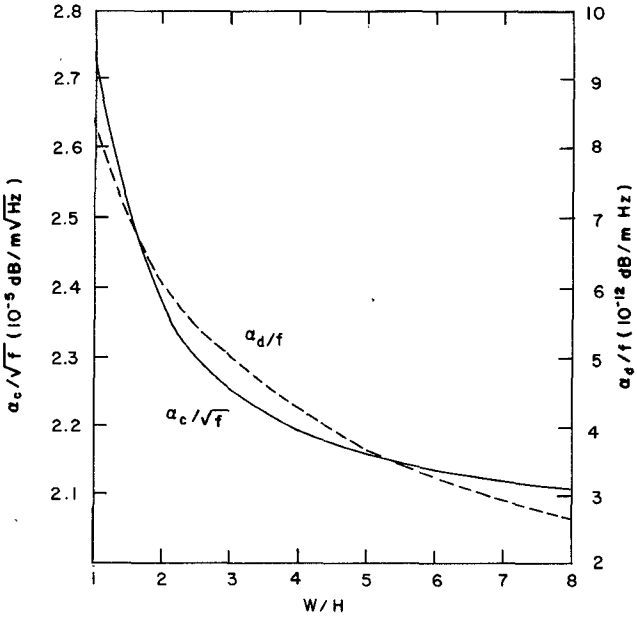

Fig. 2. Loss constants versus aspect ratio for inverted microstrip: $T = 20.0$ mils (0.508 mm), $\epsilon_1' = 3.78$, $\tilde{\epsilon}_1' = 3.88$, $\tan \delta_1 = 2.0 \times 10^{-4}$, $T_m = 0.250$ mil (6.35 μm), $\sigma = 4.10 \times 10^7$ mho/m.

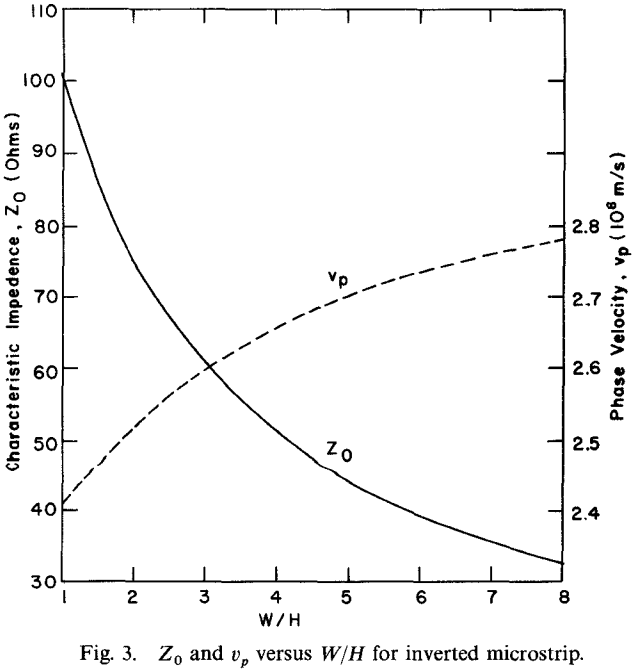

Fig. 3. Z_0 and v_p versus W/H for inverted microstrip.

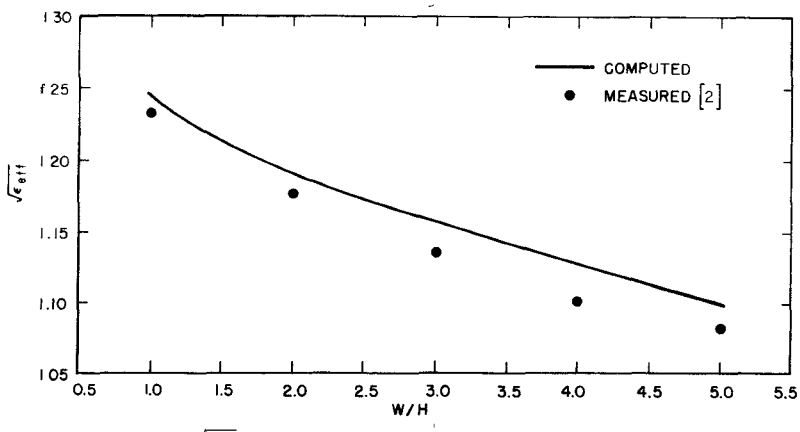

Fig. 4. Computed and measured $\sqrt{\varepsilon_{eff}}$ versus W/H characteristic for inverted microstrip: $H = 0.015$ in (0.381 mm), $T = 0.020$ in (0.508 mm), $\varepsilon_1' = 3.78$.

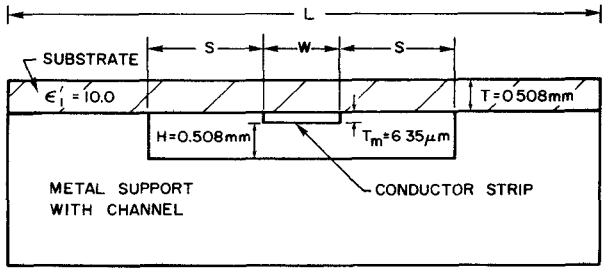

Fig. 5. Generic cross section for trapped inverted microstrip.

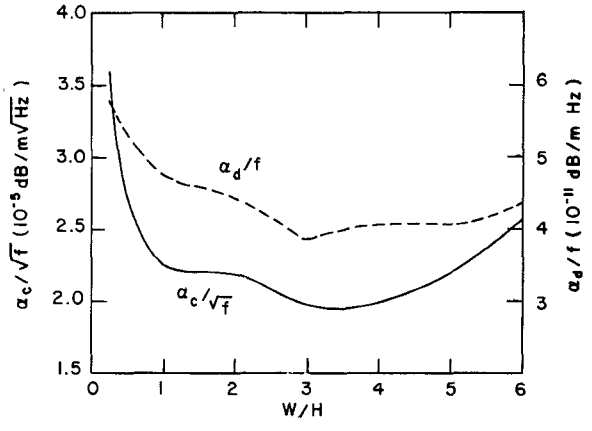

Fig. 6. Loss constants versus aspect ratio for trapped inverted microstrip: $S = 77.5$ mils (1.968 mm), $T = 20.0$ mils (0.508 mm), $\varepsilon_1' = 10.0$, $\hat{\varepsilon}_1' = 10.1$, $\tan\delta_1 = 6.0 \times 10^{-4}$, $T_m = 0.250$ mil (6.35 μm), $\sigma = 4.10 \times 10^7$ mho/m.

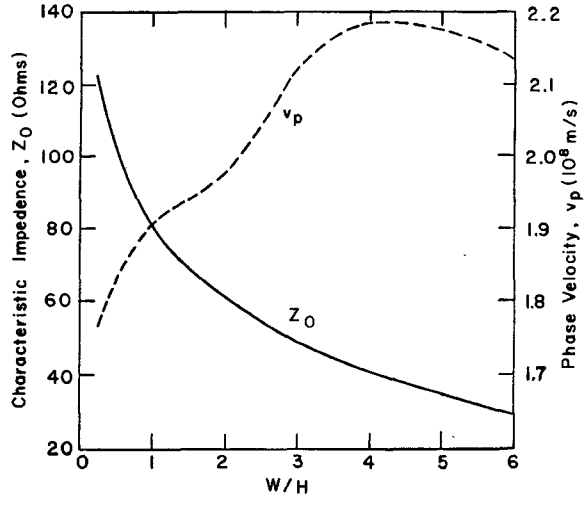

Fig. 7. Z_0 and v_p versus W/H for trapped inverted microstrip.

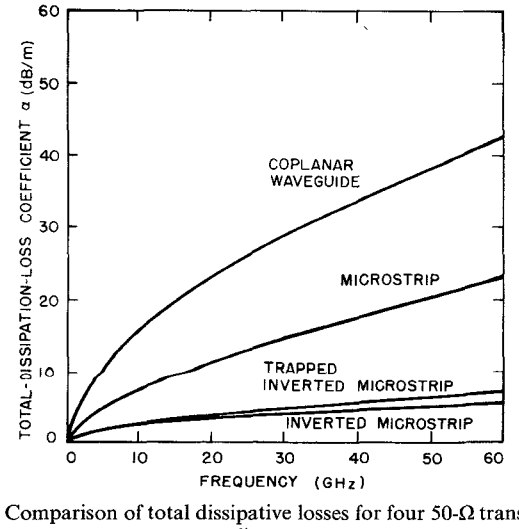

Fig. 8. Comparison of total dissipative losses for four 50-Ω transmission lines.

To demonstrate the correlation of the computed phase velocity compared to experimental data for an inverted microstrip, Fig. 4 shows computed values of $\sqrt{\varepsilon_{eff}}$ versus aspect ratio W/H as a solid curve. The measured points shown in this figure were obtained via time-domain reflectometer measurements [9]. The errors between measured and computed values are within 3 percent over this range of aspect ratios.

2) *Trapped Inverted Microstrip:* This section provides design information for trapped inverted microstrip, characterized by the generic cross-section configuration shown in Fig. 5. Calculated values of the conductor and dielectric loss coefficients are plotted in Fig. 6. The somewhat irregular appearance of these characteristics can be attributed to the effects of channel side-wall interaction with the conducting

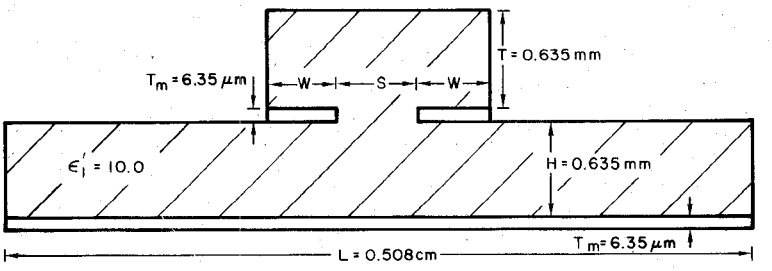

Fig. 9. Generic cross section of edge-coupled microstrip with a dielectric overlay.

strip, which is not explicitly accounted for by the "aspect ratio" definition as W/H. A similar situation is apparent in Fig. 7, where the characteristic impedance Z_0 and phase velocity v_p are shown [4].

The total dissipation loss characteristic for a nominally 50-Ω configuration of trapped inverted microstrip is plotted in Fig. 8 for comparison with those of microstrip, coplanar waveguide, and inverted microstrip.

3) Comparison of Loss Characteristics: This section presents a comparison of the loss characteristics for nominally 50 Ω, specific configurations of microstrip, coplanar waveguide, inverted microstrip, and trapped inverted microstrip transmission lines. The total loss coefficients (sum of the conductor and dielectric loss coefficients) for these lines are shown in Fig. 8 plotted versus frequency for the frequency range from 0 to 60 GHz. Effects due to higher order moding have been neglected, as well as those due to radiation losses. The curves in this figure for microstrip and coplanar waveguide correspond to configurations which are completely described in [4]. The cross-sectional configuration of microstrip chosen here represents a standard configuration of this transmission line as it has been used in many applications at frequencies up through about 12 GHz. The same is true for the selected coplanar waveguide configuration. The configuration for inverted microstrip was chosen to represent a version fabricated on a fused silica substrate, with gold being the predominant carrier of RF current in the metallization system. The trapped inverted microstrip configuration represents a model fabricated on a standard alumina substrate, metallized with a predominantly gold system. A discussion of the loss and fabrication aspects of this comparison is provided in Section IV.

B. Coupled Transmission Lines—Edge-Coupled Microstrip with a Dielectric Overlay

This section serves a twofold purpose. The first is to provide an illustrative example demonstrating the applicability of the coupled-line loss analysis developed in Sections II-B-1 and II-B-2. The second purpose is to provide a quantitative assessment of the losses encountered in quarter-wavelength long (at midband) sections of edge-coupled microstrip line with a dielectric overlay for various coupling levels.

The generic cross section of the edge-coupled microstrip with dielectric-overlay configuration is portrayed in Fig. 9.

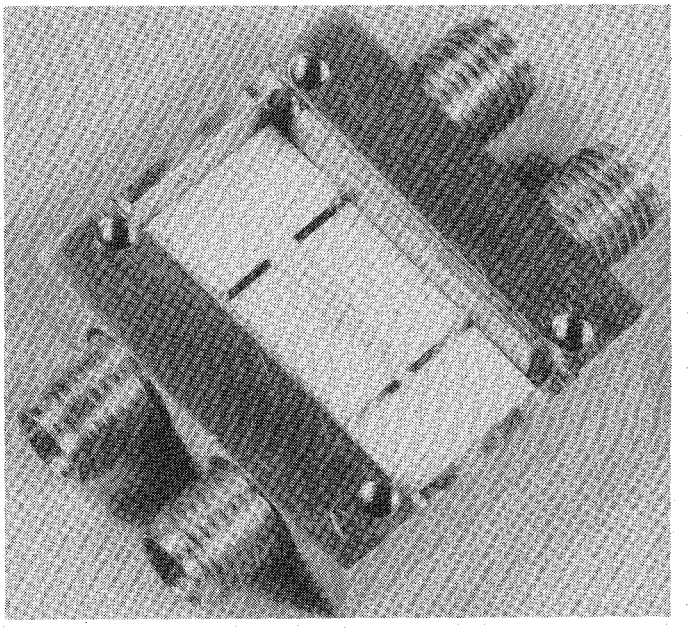

Fig. 10. Photograph of a two-section coupler employing edge-coupled microstrip with a dielectric overlay. Substrate: alumina, 0.9 × 0.4 × 0.025 in (23 × 10 × 0.635 mm). Metallization: chromium-gold, thickness = 0.00025 in (6.35 μm).

Four configurations, differing in geometric parameters were analyzed and are described in Table I. The sections numbered 1 and 2 in this table were fabricated into a two-section asymmetric coupler of the type shown in the photograph in Fig. 10. The overlays were made of alumina pieces on each section and were attached to the substrate using Stycast Hi K epoxy ($K = 10.$). The two-section coupler, over the frequency band from 2 to 8.5 GHz, had a nominal coupling value of 6.7 dB. Using (29)–(32) and the computed values of loss coefficient shown in Table I, the calculated dissipation loss for the two coupled-line sections was found to be 0.2 dB, obtained for the coupler midband frequency of 5.4 GHz. Adding in measured losses due to connectors and theoretical lead-in line loss values, the total dissipation loss determined was 0.42 dB. This agreed well with the total measured coupler dissipation of 0.4 dB.

The sections numbered 3 and 4 in Table I were combined in the fabrication of a two-section asymmetric coupler. The fabrication details of this experimental model were the same as those described for the coupler in the previous paragraph. The experimental model had a nominal coupling characteristic of 20 dB over the 2–8.5-GHz frequency band. Using an

TABLE I
PARAMETERS FOR EDGE-COUPLED MICROSTRIP WITH DIELECTRIC OVERLAY SECTIONS

SECTION NO.	W (mils / mm)	S (mils / mm)	Z_o (ohms)	Z_{oe} (ohms)	Z_{oo} (ohms)	$\alpha_{ce}/\sqrt{f}$ (dB/m) x 10^{-5}	$\alpha_{co}/\sqrt{f}$ (dB/m) x 10^{-5}	α_{de}/f (dB/m) x 10^{-10}	α_{do}/f (dB/m) x 10^{-10}
1	8.80 0.223	1.2 0.0305	50.0	115.	21.7	5.60	76.9	1.20	1.59
2	19.0 0.483	21.3 0.541	50.7	64.1	40.2	6.69	10.3	1.36	1.38
3	19.0 0.483	36.5 0.927	50.7	58.6	43.9	7.59	9.31	1.60	1.38
4	18.4 0.467	91.0 2.311	49.4	51.7	47.2	9.77	10.2	1.90	1.13

H = 25.0 mils (0.635 mm), Section Length = 0.200 in. (0.508 cm), T_m = 0.25 mil (6.35μm),

$\epsilon_1 = 10.0$, $\epsilon_1' = 10.1$

$\tan \delta_1 = 6.0 \times 10^{-4}$, $\sigma = 4.10 \times 10^7$ mho/m[10].

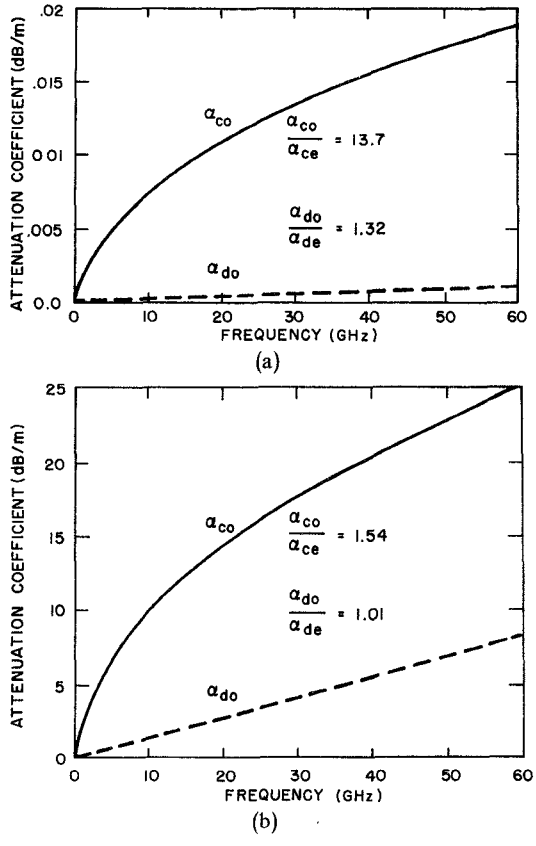

Fig. 11. Loss coefficients for sections of a 6.7-dB two-section coupler. (a) Tight section. (b) Loose section.

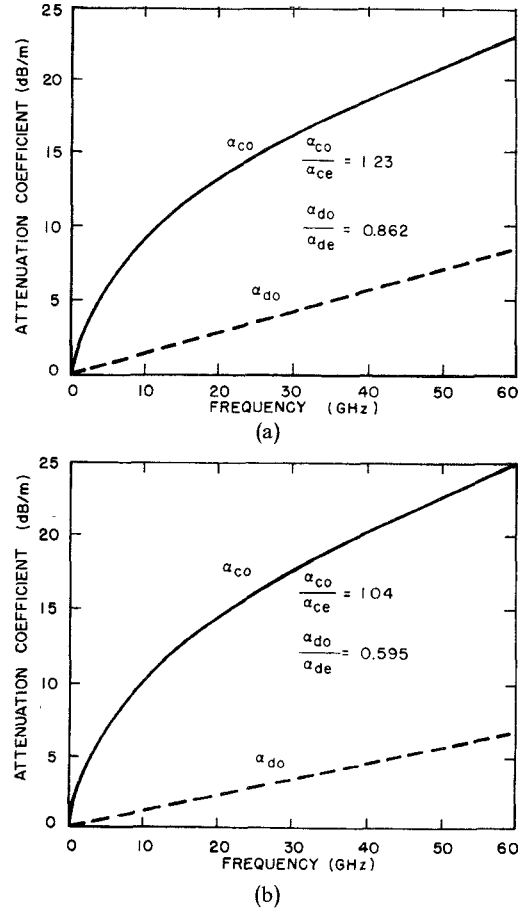

Fig. 12. Loss coefficients for sections of a 20-dB two-section coupler. (a) Tight section. (b) Loose section.

evaluation scheme similar to the one described in the previous paragraph the dissipation loss for the coupled line sections was determined to be 0.08 dB. After adding contributions for connector and lead-in line lengths the total dissipation loss was computed to be 0.38 dB. This agreed well with the measured midband (5.4 GHz) dissipation loss of 0.4 dB.

Another portrayal of the loss characteristics computed for these four coupled-line sections is shown in Figs. 11 and 12. Fig. 11 shows plots of α_{co} and α_{do} versus the frequency for the tight (section number 1) and loose (section number 2) coupling sections used in the 6.7-dB coupler. Also shown are the ratios α_{co}/α_{ce} and α_{do}/α_{de}. It is interesting to note the large disparity between the even- and odd-mode conductor losses for the tight section. Fig. 12 shows similar data for the tight (section number 3) and loose (section number 4) coupling sections used to make up the 20-dB coupler.

IV. Discussion

This paper details and illustrates analyses, amenable to computer programming, which can be used to evaluate dissipation losses in isolated or coupled microwave and millimeter-wave transmission lines. These lines can be composed of both imperfect conductors and piecewise-homogeneous dielectric materials. The analyses described here have been implemented in the form of digital computer programs [4] for treating: microstrip, coplanar waveguide, inverted microstrip, trapped inverted microstrip, and edge-coupled microstrip with dielectric overlay.

The programs for microstrip and coplanar waveguide were used to analyze a variety of configurations for these transmission lines. The computed values of conductor loss for microstrip on alumina have been compared [4] with the well-accepted values of Schneider [9] and were found to agree within better than 1.6 dB/m for frequencies up through 18 GHz. The computed values for dielectric losses in microstrip agree with Simpson *et al.* [11] and Schneider [12] and agreed to within 3 percent or better at frequencies up to 18 GHz. Computed total loss constants for microstrip have been compared with the results of Pucel *et al.* [13] and Gopinath *et al.* [14] and agree to within 0.01 dB/cm over the frequency ranges cited in these references. The sum of conductor and dielectric losses computed for coplanar waveguide agreed with the experimental values of McDade and Stockman [15] to within 0.1 dB/wavelength. The experimental determinations were made by two independent techniques.

Conductor and dielectric loss coefficients were also evaluated and presented here for inverted microstrip and trapped inverted microstrip. This information was presented in the form of useful design curves, providing loss values as functions of the aspect ratios for these lines. It was encouraging to note the agreement (better than 2 percent) of the computed phase velocities $\sqrt{\varepsilon_{\text{eff}}}$ for inverted microstrip when compared to measured data [9]. These calculations are made using the same equivalent charge densities that are used in the loss calculations.

A comparison of computed total loss coefficients for the four types of lines just discussed is shown in Fig. 8. It is interesting to note that the losses incurred in inverted and trapped inverted microstrip at frequencies as high as 60 GHz are comparable to those incurred in microstrip for frequencies in the 5–10-GHz frequency range. It is also seen that coplanar waveguide appears to be considerably more lossy than microstrip. The structures compared in this figure were selected to have characteristic impedance levels of nominally 50 Ω. Consistent with this characteristic, the conducting strip widths required for microstrip and coplanar waveguide were approximately two and one half to three times narrower than those required for inverted and trapped inverted microstrip. This feature enhances the attractiveness of the inverted and trapped inverted microstrip lines by virtue of the mitigation of fabrication difficulties. By concentrating more of the field energies in air (with correspondingly lower ε_{eff}), wider strips are possible for a prescribed impedance level (compared to the other two lines). These advantages should be realized even if the dimensions must be contracted to suppress higher order moding at higher frequencies. This should be investigated more extensively. Also, it should be noted that the transmission lines shown in Figs. 1, 5, and 9 may have to be shielded for some practical circuit applications.

The analyses for computing conductor and dielectric loss coefficients and for relating these parameters to terminal-electrical characteristics were applied to edge-coupled microstrip with a dielectric overlay. Computed results were compared to measured characteristics for two experimental models of two-section couplers, having nominal coupling values of 6.7 and 20 dB, respectively. The total dissipation values computed for these couplers agreed with experimental evaluations within 0.07 dB.

It is interesting to note that the difference between the even- and odd-mode loss coefficients for this structure gives rise to a finite isolation for an otherwise perfect coupled-line section. For the 6.7-dB coupler considered here, the tight and loose sections are limited to maximum isolation levels of 42 and 59 dB, respectively, due to this phenomenon. The tight and loose sections of the 20-dB coupler are similarly limited to 70- and 92-dB isolation levels, respectively.

There are several factors which can contribute to error in the analyses described here. One is the discrete representation of charge-density distributions employed in the quasi-TEM model employed. In one sense, this discretization can be viewed as a "surface roughness" which could lead to a high estimate of losses. Mathematical smoothing of the charge-density distributions might lead to improvement. An approach which could improve the accuracy is to solve the magnetostatic problem to evaluate the magnetic field at conductor surfaces for these transmission media. Certainly the difference quotient approximation used to arrive at (15) introduces error in the dielectric loss evaluations. Also, judicious choices must be made for the dc conductivity of the metal system and the loss tangents for dielectrics.

Acknowledgment

The author extends his sincere thanks to Ms. Rosemary Kelly for preparing the manuscript for this paper.

References

[1] B. E. Spielman, "Analysis of electrical characteristics of edge-coupled microstrip lines with a dielectric overlay," Naval Research Laboratory, Washington, DC, NRL Rep. 7810, Oct. 25, 1974.

[2] R. F. Harrington *et al.*, "Computation of Laplacian potentials by an equivalent source method," *Proc. Inst. Elec. Eng.*, vol. 116, no. 10, pp. 1715–20, Oct. 1969.

[3] R. F. Harrington, *Time-Harmonic Electromagnetic Fields.* New York: McGraw-Hill, 1961, pp. 61–67.

[4] B. E. Spielman, "Computer-aided analysis of dissipation losses in isolated and coupled transmission lines for microwave and millimeter wave integrated circuit applications," Naval Research Laboratory, Washington, DC, NRL Rep. 8009, July 1976.

[5] J. D. Jackson, *Classical Electrodynamics.* New York: Wiley, 1966, pp. 236–240.

[6] R. F. Harrington, *Time-Harmonic Electromagnetic Fields.* New York: McGraw-Hill, 1961, p. 50.

[7] Leo Young, Ed., *Advances in Microwaves*, Vol. 1. New York: Academic Press, 1966, pp. 115–209.

[8] B. Sheleg and B. E. Spielman, "Broad band directional couplers using microstrip with dielectric overlays," *IEEE Trans. Microwave Theory Tech.*, vol. MTT-22, pp. 1216–1220, Dec. 1974.
[9] M. V. Schneider, "Microstrip lines for microwave integrated circuits," *BSTJ*, vol. 48, no. 5, pp. 1421–1444, May–June 1969.
[10] C. D. Hodgman, Ed., *Handbook of Chemistry and Physics*. Cleveland, OH: Chemical Rubber Publishing Co., 1961, p. 2628.
[11] T. L. Simpson and B. Tseng, "Dielectric loss in microstrip lines," *IEEE Trans. Microwave Theory Tech.*, vol. MTT-24, pp. 106–108, Feb. 1976.
[12] M. V. Schneider, "Dielectric loss in integrated microwave circuits," *BSTJ*, vol. 48, pp. 2325–2332, Sept. 1969.
[13] R. A. Pucel, D. J. Masse, and C. P. Hartwig, "Losses in microstrip," *IEEE Trans. Microwave Theory Tech.*, vol. MTT-16, pp. 342–350, June 1968.
[14] A. Gopinath, R. Horton, and B. Easter, "Microstrip loss calculations," *Electron. Letts.*, vol. 6, no. 2, pp. 40–41, Jan. 22, 1970.
[15] J. McDade and D. Stockman, "Microwave integrated circuit techniques," AFAL/TEM, Wright Patterson AFB, OH, Tech. Rep. AFAL-TR-73-234, May 1973.

Analysis of Distributed-Lumped Strip Transmission Lines

TADAHIKO SUGIURA

Abstract—**A calculation method for obtaining characteristic impedances and phase velocities of striplines, which are regarded as consisting of distributed-lumped elements such as so-called wiggly lines, is presented with numerical results. The numerical calculations have been carried out for a) single stripline with slots at the outer edges, b) coupled stripline with rectangular wiggling, and c) coupled stripline with slots at the outer edges. Experimental work has also been accomplished to verify the present method. Results show good agreement with calculations.**

I. Introduction

RECENTLY, stripline circuits have become widely used at microwave frequencies, in accordance with microwave integrated circuit developments. Parallel coupled striplines are especially useful for realizing filters, directional couplers, and other microwave circuits.

In an ordinary coupled line, shown in Fig. 1(a), the phase velocities of the even and odd modes differ because of the inhomogeneity of the ambient medium. The difference in the two velocities usually causes undesired degradation of the circuits. Podell has solved this problem by introducing the wiggling technique [1]; that is, wiggling the coupled edges as shown in Fig. 1(b). Due to the different distributions of the even and odd mode currents, it is possible to raise the odd mode inductance more than the even mode inductance by the wiggling technique. Generalizing this idea, deRonde has shown that a tightly coupled line can be realized by slotting the outer edges of the wiggly line, as shown in Fig. 1(c) [2]. These lines can be regarded as consisting of distributed-lumped elements. The inductance or the capacitance of a stripline may be widely varied by applying the above-mentioned distributed-lumped technique.

For practical applications, however, tedious cut-and-try experiments are needed to obtain the desired value, because available experimental data are very scarce and no quantitative analysis has been reported for these lines. This paper presents a calculation method to obtain the characteristic impedance and the phase velocity of the distributed-lumped striplines. Numerical results obtained with the aid of a digital computer are compared with experimental data.

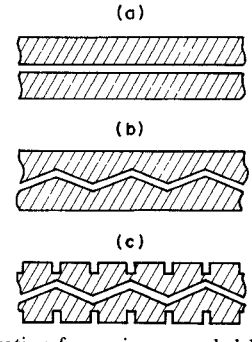

Fig. 1. Strip configuration for various coupled lines: (a) ordinary line, (b) and (c) distributed-lumped lines.

II. Theory

A. General Considerations

The distributed-lumped stripline has a periodic structure, as shown in Fig. 2. On the assumption that one unit section of the periodic structure is much shorter than the wavelength, static theory can be applied for determining the inductance and the capacitance per unit section, because the voltage and the current are regarded as constant over the unit section. If the inductance and the capacitance are obtained, the characteristic impedance and the phase velocity are readily calculated, according to ordinary transmission line theory. Accordingly, the problem is reduced to calculations of the inductance and the capacitance per unit section.

Although various types of line structure can be considered in distributed-lumped lines, the calculation model chosen is

Manuscript received August 15, 1973; revised January 21, 1977.
The author is with the Central Research Laboratories, Nippon Electric Company, Ltd., Kawasaki 213, Japan.